Invited Paper

The Femtoprint Project

Y. Bellouard[1,*], A. Champion[1], B. Lenssen[1], M. Matteucci[1], A. Schaap[1], M. Beresna[2], C. Corbari[2], M. Gecevičius[2], P. Kazansky[2], O. Chappuis[3], M. Kral[3], R. Clavel[3], F. Barrot[4], J.-M. Breguet[4], Y. Mabillard[5], S. Bottinelli[5], M. Hopper[6], C. Hoenninger[7], E. Mottay[7], J. Lopez[8]

[1] *Mechanical Engineering Department, Eindhoven University of Technology, Eindhoven, The Netherlands*

[2] *Optoelectronics Research Center (ORC), University of Southampton, Southampton, United Kingdom*

[3] *LSRO, Ecole Polytechnique Fédérale de Lausanne, Lausanne, Switzerland*

[4] *Centre Suisse d'Electronique et Microtechnique (CSEM), Neuchâtel, Switzerland*

5 Mecartex, Losone, Switzerland

[6] *Quintenz Hybridtechnik, Neuried bei München, Germany*

[7] *Amplitude Systèmes, Pessac, France*

[8] *AlphaNOV, Talence, France*

**Corresponding author, email: y.bellouard@tue.nl*

The Femtoprint project, a European project, aims at demonstrating the use of low-energy laser pulses (i.e. below the ablation threshold) to manufacture monolithically integrated devices including optofluidic, optomechanical and photonic devices. The longer-term objective is the implementation of a versatile table-top machining center. This paper summarizes the project progress to date and demonstrates the potential of this approach through various illustrative examples.

DOI:10.2961/jlmn.2012.01.0001

Keywords: Femtosecond lasers, nanogratings, optofluidics, optomechanics, photonics devices.

1. Introduction

1.1. Functional integration at the microscale

The last decades have seen the emergence of micro-/nano-systems with diverse functionalities (see Figure 1). Starting from integrated circuits in the 1970's, followed by micro-mechanical systems in the 1980's-1990's, photonics and fluidics in the 1990's-2000's and recently the addition of organic material and bio-molecules, micro-/nano-systems are becoming complex machines performing sophisticated tasks.

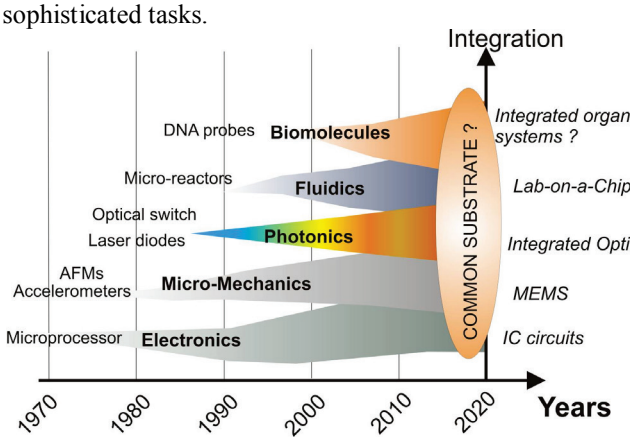

Fig. 1 The road to system integration.

Significant progress and breakthroughs are expected with the integration of these functionalities on a common platform. While the merger of electronics and micro-mechanics on a common platform (MEMS) is showing significant success, a true integration of photonics, micro-mechanics and fluidics on a common platform has yet to be successfully demonstrated and implemented.

This is especially true when working with non-planar (i.e. 3D) devices. Despite undisputable successes - vivid examples are accelerometers or inkjet printer heads - the number of successful microsystem applications (i.e. that get out of the laboratory) remain limited and below the perceived potential. One well-known bottleneck in the fabrication of microsystems combining multiple functionalities as diverse as fluidics, optics and mechanics is the packaging and the ever increasing complexity of fabrication processes.

Progress in that field could be made by applying disruptive design concepts and processes that we briefly introduce in the next paragraph.

In addition to the technical limitations mentioned above, classical microfabrication approaches face economical and societal issues. The spectacular miniaturization trend ongoing for the last thirty years in various fields has not been paralleled by a similar miniaturization of the production means. Ironically, today, the microsystems industry uses large numbers of sophisticated equipment to fabricate very small parts. Large capital investments are required to set up and operate such microsystems production facilities. Consequently, mainly products with potentially large markets (such as accelerometers) are considered, and only a few large suppliers can make the necessary financial investments. Small and medium size companies are prevented from entering the field although they usually are a strong source of innovative ideas. This issue has a negative impact on our innovation capabilities as well as our abilities to rapidly adapt to new demands.

Further, foundries where surface micromachining takes place consume large amount of energy, most of it being wasted in operating the machinery and in the control of air temperature, humidity and purity as required for photolithography [1], [2]. As sustainable growth requirements become more prevalent, these power-hungry fabrication techniques will face increasing societal scrutiny.

Alternative production methods that can bypass some these issues will be of increasing interest. One of these new approaches is the use of femtosecond lasers to fabricate glass based integrated microsystems, sensors and photonics devices.

1.2. Effect on glass exposed to low-energy femtosecond laser pulses

Recent progress in femtosecond laser micromachining of fused silica have made possible the fabrication of integrated optics (from first demonstrations [3][4][5][6], to complex integrated optical systems [7][8]), optical data storage [9], new optical components [10][11], microchannels [16], and a combination of both [13] [40][14][15][18], and all-glass optomechanical devices [21]. Thanks to the broad number of functions that can be integrated in a single piece of material [23], fused silica processing with femtosecond laser has become the ideal platform for monolithic integration.

1) The material is selectively exposed by rasterizing a pattern according to a technique described in [16].

2) After laser-exposure, the part is etched in a low-concentration HF bath. Concentrations between 2.5% and 5% are typically used. Etching time depends on pattern sizes and varies from one hour to several hours for the deepest structures. Following etching the part is rinsed in de-ionized water and dried.

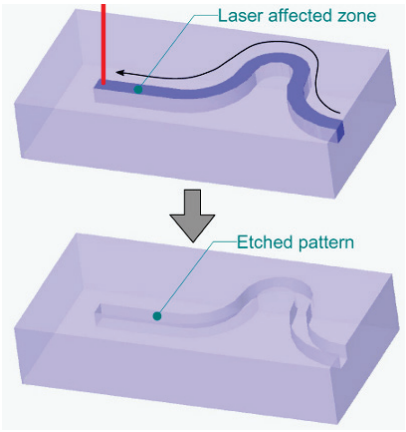

Fig. 2 Illustration of the two-step microfabrication process to process fused silica using femtosecond laser exposure combined with chemical etching.

1.3. The Femtoprint project

The Femtoprint project is a European project aiming at providing simple, affordable and on-site microsystem and photonic devices production capabilities to a large community of users. Specifically, it explores the use of low-energy femtosecond pulses for fabricating micro- and nano-scale devices in glass materials. These microsystems will have the capability to combine structural features (for instance for fluid or gas handling) with optical functionalities and micromechanical functionalities.

Although enormous instantaneous powers are locally reached (Gigawatts or even Terawatts per cm^2) during the laser exposure, the average power typically does not exceed a few hundred of milliwatts, which is comparable to what a bright LED emits. Thanks to this low average power requirements, femtosecond lasers consisting simply of an oscillator are sufficient to produce complex micro- and nano- systems. These laser systems are nowadays table-top and cost a fraction of the cleanroom equipment needed for producing similar structures. It is foreseeable that within 5 years the size of such laser systems can be reduced to a shoe-box.

One objective of Femtoprint is to develop a printer for micro-/nano-sytems fabricated out of glass. Fig. 3 shows an artistic view of the 'femtoprinter' (with realistic dimensions with respect to the computer) under development.

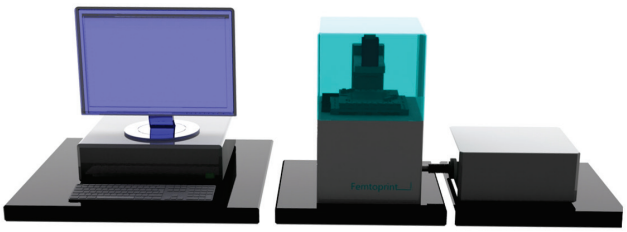

Fig. 3 Artistic view of the prototype Femtoprinter. The system consists of a control unit, a laser scanning system (central part) and the laser source (right).

The system consists in three units: the control unit, the laser scanning system and the laser source. The laser source is an oscillator whose specifications are shown in Table 1.

Table 1 Preliminary Femtoprinter laser source specifications

Parameters	Value
Pulse duration	200-500 fs
Pulse energy	< 1uJ
Repetition rate	0-5MHz

The moderate to low pulse energy reduces the laser requirement in term of power dissipation and size but is nevertheless sufficient for selectively modifying the glass matrix structure. The repetition rate is chosen to cover the domain of energy where no or little cumulative effects are observed.

2. Process optimization

It was recently shown [43] that the net deposited energy (i.e. the energy effectively deposited in a given volume element) plays a key role in deciding the etching rate of laser processed bulk fused silica. There is an optimum deposited energy to achieve maximum etch rate. This is illustrated in Figure 4. This net deposited energy is directly dependent on the scanning speed and the repetition rate. It is therefore possible to define an optimum processing window for which the fastest etching rate (and as a consequence, the highest aspect ratios) are obtained.

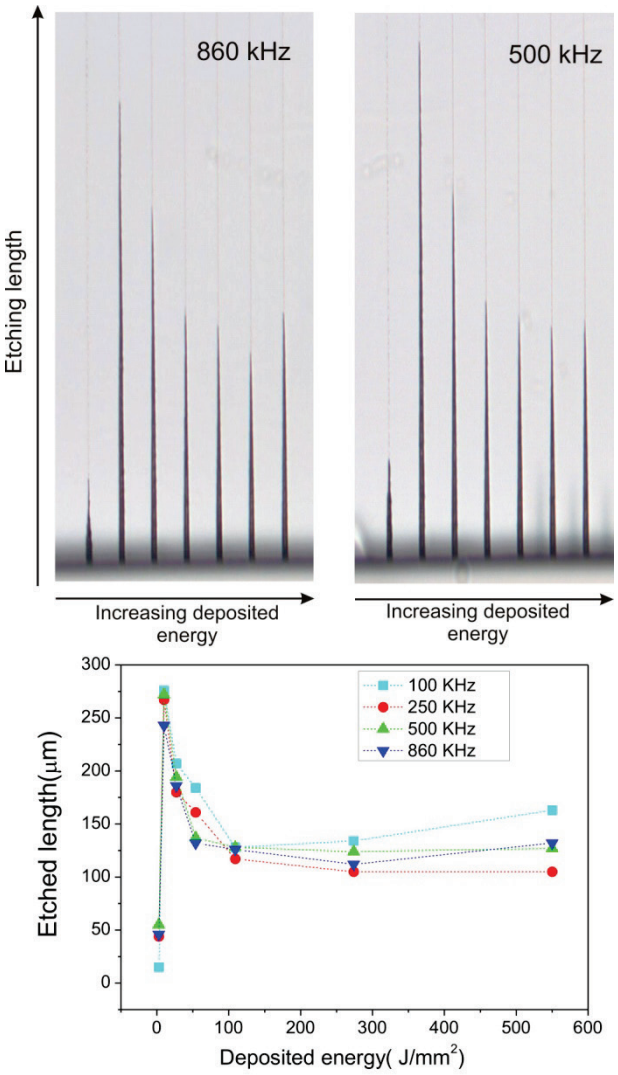

Fig. 4 Effect of deposited energy. The top image shows buried lines partially etched for increasing deposited energy and for two repetition rates. The etching length as a function of the deposited energy shows evidences for an optimum processing window [43].

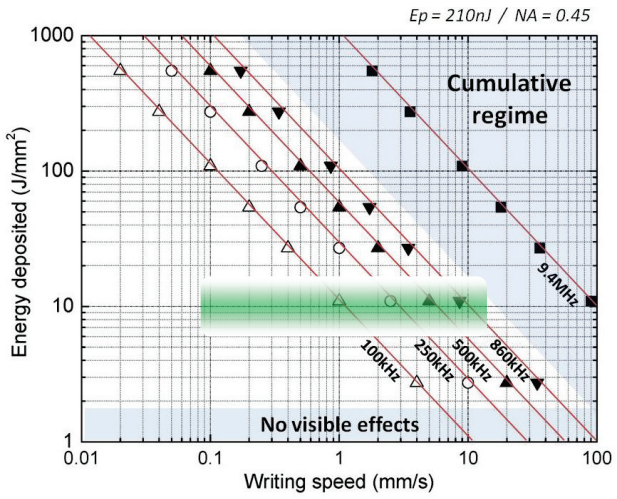

Fig. 5 Optimum process window for pulse energy of 210 nJ and a given set of confocal parameters and laser exposure conditions (pulse duration =380 fs). The optimal machining regime with these confocal parameters is shown (green frame).

An example of such processing window is shown in Figure 5. This results are given for a pulse energy of 210 nJ and for a femtosecond laser emitting 500 fs-long pulses at 1030 nm. In this configuration, it is found that the optimal level of deposited energy is around 10 J/mm^2. For this value, an appropriate ratio between repetition rate and scanning speed can be selected to optimally expose the silica material.

3. Illustrative examples / Applications

The femtoprint process finds numerous applications, in particular in the fields of optofluidics, optomechanics, photonics, and micromolding, as well as marking and information storage. In this section, we present a few illustrative examples.

3.1. Three-dimensional machining and sub-wavelength manufacturing

Thanks to the non-linear nature of the ultrafast laser-matter interaction, the energy is locally absorbed wherever the laser spot is focused. In transparent materials such as dielectrics, the laser can be focused anywhere inside the material and the energy can be deposited anywhere in the volume. Using this property, it is therefore possible to create three-dimensional structure as long as there exists a path for the etchant to penetrate in the laser affected regions. Various authors have demonstrated the fabrication of three-dimensional objects using this principle (see for instance [28], [29]). Figure 6 shows another example made in fused silica and using the femtoprinter parameters.

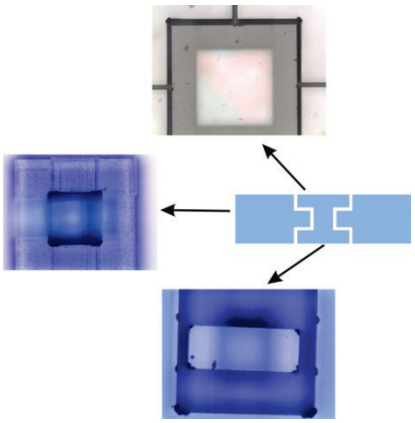

Fig. 6 Illustration of a three-dimensional multi-layer structure.

It consists of a multi-layer structure that is separated from the substrate but yet remains encapsulated inside the substrate. This simple example demonstrates the unique advantage of the use of femtosecond laser compared to more traditional lithographic techniques that is its three-dimensional capability.

While traditional industrial laser-machining processes based on melting processes see their smallest feature size driven by the optical diffraction limit and as such cannot typically be smaller than the laser wavelength itself, the non-linear laser-matter interaction taking place when using an ultra-fast laser offers the possibility to produce features below the diffraction limit. To illustrate this important properties, Fig. 7 shows a nanoscale channel that was manufactured with a femtosecond laser emitting at 1030 nm.

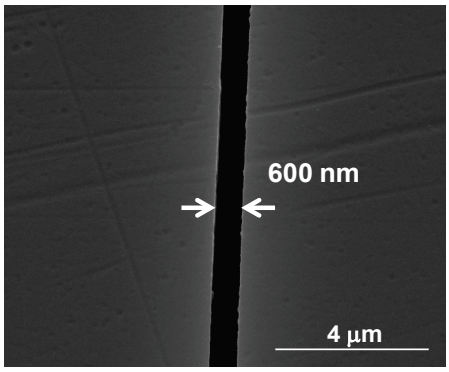

Fig. 7 Illustration of a nanoscale microchannel. This example demonstrates that, thanks to the non-linear absorption properties inherent in the use of an ultrafast laser, features smaller than the wavelength of the laser itself (here 1030 nm) can be fabricated.

Another remarkable example of sub-wavelength structures was shown by Shimotsuma *et al.* [27]. In their seminal work, they demonstrated the formation of nanogratings, i.e. self-organized features of nanometer sizes appearing in the laser spot itself.

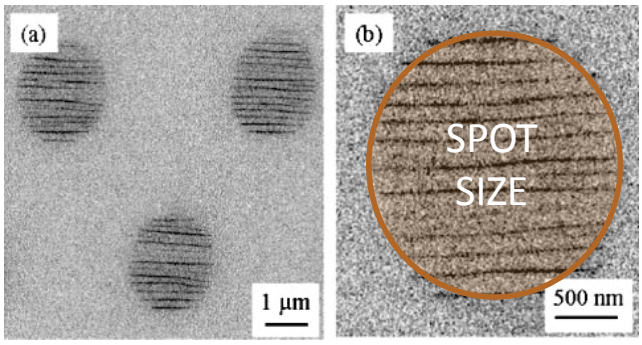

Fig. 8 SEM images of nanogratings forming in laser affected zones. (Images inspired from [27]).

3.2. Optomechanical devices

Although counterintuitive at first, fused silica is an interesting platform for developing integrated optomechanical devices. The material has excellent mechanical properties provided that its surface properties are controlled. Here, the use of an etching step greatly improve the mechanical properties, and high-strength elastic elements such as flexures can be produced [22]. The simulataneous integration of optics and mechanics in a single substrate was demonstrated in [21].

This concept can be pushed further by introducing actuating properties. This can be realized using a comb-array design (as shown in Fig. 9). Once it is coated with an electrode (which using ITO can be transparent), the comb-array behaves like a capacitor and can be used as a sensor or as a force generator upon application of a voltage. The femtoprint process creates structures with aspect ratio comparable or higher than competetive processes like Deep Reactive Ion Etching (DRIE). It is therefore particularly suitable for the design of in-plane mechanisms such as the mechanism presented in [21] or the one shown in Fig. 9.

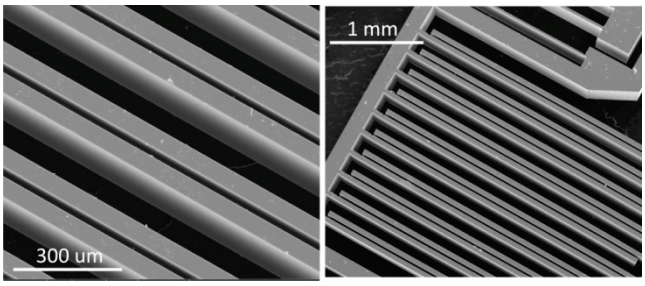

Fig. 9 Scanning electron microscope images close-up views of the fabricated comb-array actuator.

3.3. Photonics devices

Beams with radial or azimuthal polarization are of particular interest due to their high inherent symmetry and the unique optical properties. Such beams enable resolution below the diffraction limit [30] and interact more efficiently with materials [31] without the undesirable anisotropy observed with linearly polarized light. They also have a relatively large longitudinal component of electric field which is promising for applications such as particle acceleration. However, current methods of polarization manipulation require specialised and expensive equipment. Furthermore limits on the throughput power rules out applications such as material processing and particle acceleration. However, it has been demonstrated that polarization can be successfully manipulated with the help of form birefringence associated with sub-wavelength gratings [32]. Additionally, it was found that the femtosecond laser direct writing can be employed for this task. Moderate fluencies of ultrashort laser irradiation lead to spontaneous formation of self-assembled nanogratings, which behave as negative uniaxial crystals, with the slow and fast optical axes aligned respectively parallel and perpendicular to the grating corrugation [33]. Earlier works reported results on birefringence produced by self-assembled nanogratings [34][35] that can also be used, as recently reported, for the fabrication of quarter- and half-waveplates [36]. Recently, polarization gratings imprinted by femtosecond laser nanostructuring have been demonstrated [37]. This method can be successfully implemented for the fabrication of polarization converters to create arbitrary polarization states, including polarization vortexes.

The most straightforward approach is conversion of circularly polarized light into radial/azimuthal polarization. By using Jones calculus we can describe a polarization converter element. Multiplying a vector describing left handed circular polarization by the Jones matrix of polarization converter we obtain the following expression:

$$\begin{pmatrix} \cos^2\theta + i\sin^2\theta & (1-i)\cos\theta\sin\theta \\ (1-i)\cos\theta\sin\theta & i\cos^2\theta + \sin^2\theta \end{pmatrix} \frac{1}{\sqrt{2}} \begin{pmatrix} 1 \\ i \end{pmatrix} = \begin{pmatrix} -\sin\phi \\ \cos\phi \end{pmatrix} e^{i\phi} e^{i\frac{\pi}{4}},$$

where the angle $\theta = \phi + \pi/4$ and ϕ is the polar angle. Neglecting constant phase shift we see that the resultant electric field has azimuthal orientation and it possess orbital angular momentum $l = 1$. Alternatively, right handed circular polarization will produce radially polarized beam with orbital angular momentum $l = -1$. Thus space variant phase

of the converter can form a beam with the orbital angular momentum [38], where its sign is controlled with the handedness of incident circular polarization.

The experimental setup used to imprint the polarization converter was composed of a PHAROS mode-locked regenerative amplified Yb:KGW based femtosecond laser system (Light Conversion Ltd.) operating at $\lambda = 1030$ nm and delivering pulses of 270 fs at a 40 kHz repetition rate. The beam was focused with a low numerical aperture Nachet ×20 objective (NA = 0.35) into a 2 mm thick fused silica plate 200 μm below the surface. In our experiments we observed retardance as high as 260 nm after a single pass of writing laser beam which enables us to fabricate efficient polarization converters working in the visible and near infrared. The laser beam polarization azimuth was manipulated by an achromatic half-wave plate mounted on a motorized rotation stage.

To verify presence of radial polarization the converter was inserted into the path of a monochromatic circularly polarized beam and the light at the exit was observed with or without the linear polarizer [38]. The propeller shape (which is typical for radial polarization) observed through linear polarizer under optical microscope confirmed successful implementation of birefringent polarization converter.

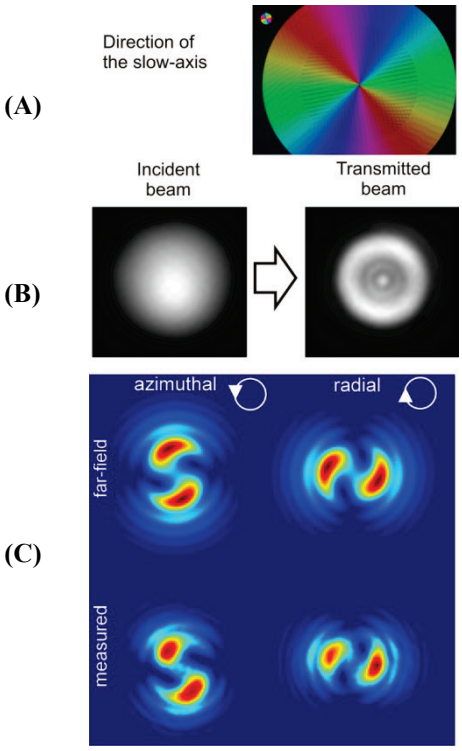

Fig. 10 Illustration of a photonic device made using a femtosecond laser. This device is a polarization converter that turns a circularly polarized beam into a radially polarized one [11]. The pattern (A) (whose directions of slow-axis are shown in the top image) consists of a circular disk of femtosecond laser marks with gradually change the slow-axis orientation. The middle image (B) shows how the energy distribution of an incident Gaussian beam is modified after passing through the device. The bottom image (C) shows a comparison between the simulated field distribution and the measured one for both, radial and azimuthal polarization.

Constant value of retardance with continuously varying direction of the slow axis was measured across the whole structure. The optical properties of the polarization converter were tested with a continuous-wave Nd:YAG laser second harmonic ($\lambda = 532$ nm). The transmission losses are 40 % in the green, 20 % at 1 micron and 10 % in the telecom wavelengths. The measurements made in the far-field were found to be in good agreement with the model this optical system based on Jones matrix formalism and Fourier propagation.

The technique enables achieving radial or azimuthal polarizations simply by controlling the handedness of incident circular polarization. More complex polarization converters can be easily designed by controlling polarization of the writing femtosecond laser beam.

3.4. Micro-molding

Micro-molding can be used for the cost-effective fabrication of elements such as active or passive components in MEMS devices, hydrophobic surfaces, cell-growth scaffolds or optical components such micro-lens arrays and gratings.

The three-dimensional capabilities of the process makes it suitable for the fabrication of micromolds used for the fabrication of low-cost polymer replicas. In [44], we demonstrated the process of such molds. Noteworthily, this method is also particularly interesting for examining high-aspect ratio laser-machined structures fabricated in glass material. Thanks to this technique, surfaces not accessible with common imaging techniques can be observed on their molded negative structure with very high fidelity.

The steps for the preparation of three-dimensional molds using femtosecond laser processing and etching are shown in Fig. 11. The first two steps are the laser exposure and the chemical etching using the lasers and methods discussed in the previous paragrahs.

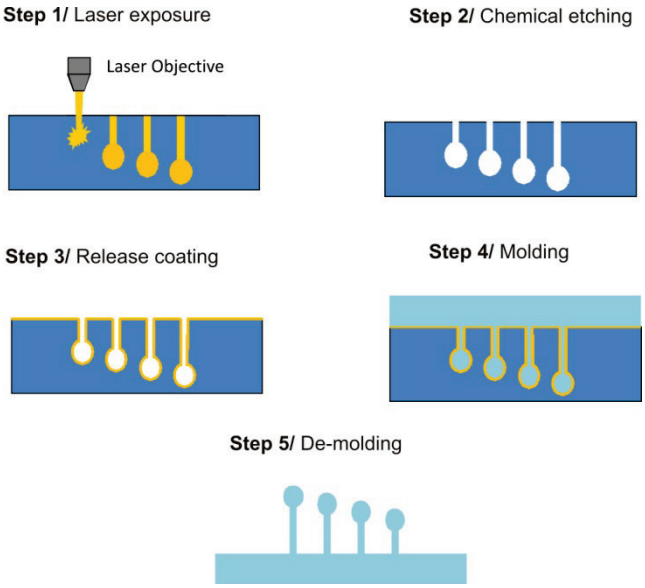

Fig. 11 Micro-molding of femtosecond laser micromachined structures. The first two steps are the machining per se. A key aspect of this molding procedure is the use of a release coating that reduces the polymer adhesion and friction with the glass substrate. The process is described in great detail in [44].

To reduce both the adhesion of the molding material to the mold and the friction experienced by the molding upon release, a 20 nm thick, densely packed, irreversibly adsorbed polydimethylsiloxane monolayer is grown on clean, hydroxyl-rich silica substrates (step 3). The final result is obtained through a physisorption mechanism involving mainly multiple H-bonding. The nanocoating's high packing density, together with the low surface tension and friction coefficient of PDMS (liquid at room temperature with extremely mobile chains) make for an effective release coating.

After performing the monolayer deposition, a uniform mixture of PDMS base and cross-linker (Sylgard 184) (or other polymer depending on the application) is poured onto the substrate to generate negative PDMS templates. The percentages of base and cross-linker are chosen to give rise to elastomers optimized from a mechanical standpoint (relatively high stiffness and ultimate tensile strength while being highly compliant). The final step is the demoulding proper.

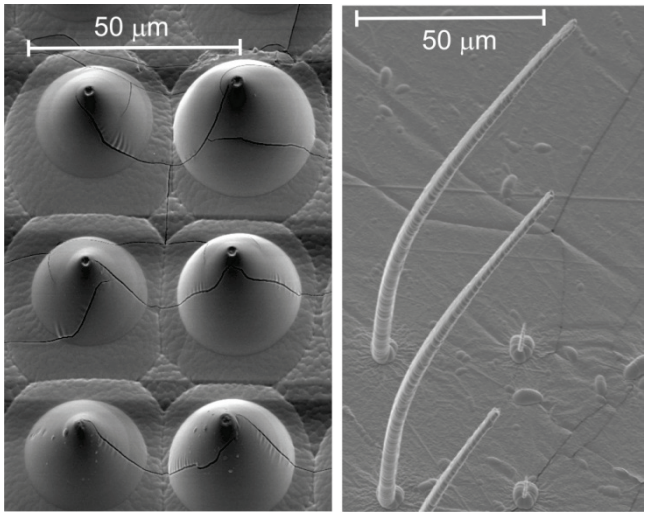

Fig. 12 Left: Moldings of Borofloat conical holes. Right: Moldings of long narrow holes made in fused silica. The demolded structures (standing up on the substrate) are more than 100 µm long.

Fig. 12 shows two illustrative examples of molded femtosecond micromachined substrates. The left example is a borofloat glass on which conical structures were formed after etching of straight vertical lines written with the femtosecond laser. The cracks visible on the image are artefacts from the sample preparation and comes from the metal coating necessary for a proper SEM image formation. The right image shows very long self-standing structures of PDMS after the release from the glass substrate. These pillars are more than 100 µm long and a few microns wides. This demonstrates the high-aspect ratio capability of this micro-molding approach.

3.5. Optofluidics

The simultaneous fabrication of integrated optics and microstructures is of particular interest for optofluidics [12]. Since pioneer works (see for instance [13], [14], [17] and ref [19], [20] that provide overview of the field), there have been various demonstrations made of labs-on-a-chip integrating waveguides and fluidic channels. Here, we show an illustration of femtosecond fabricated biochip for the rapid identification of algae [18].

The rapid identification of algae species is not only of practical importance when monitoring unwanted adverse effects such as eutrophication, but also when assessing the water quality of watersheds. In [18], we demonstrated a lab-on-a-chip that functions as a compact robust tool for the fast screening, real-time monitoring, and initial classification of algae. The water-algae sample, flowing in a microfluidic channel, is side-illuminated by an integrated subsurface waveguide.

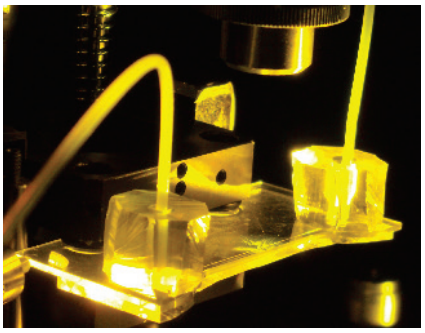

Fig. 13 Example of biochip for algae population monitoring. The biochip is made out of a single piece of glass on which are attached two PDMS connectors and a removable cover to seal the channel.

The waveguide is curved to improve the device sensitivity. The changes in the transmitted optical signal are monitored using a quadrant-cell photo-detector. The signal-wavelets from the different quadrants are used to qualitatively distinguish different families of algae (see Fig. 14).

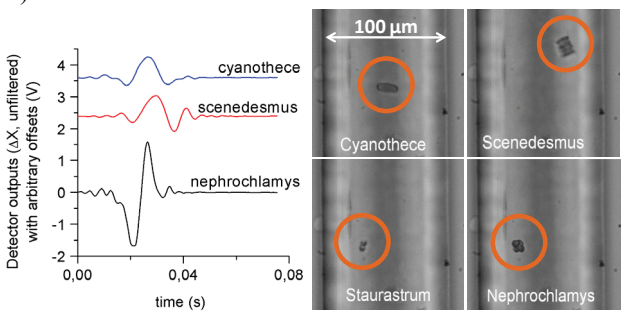

Fig. 14 (left) Examples of wavelets signals obtained for specific algae species. (right) Images captured on the fly by a microscope camera overlooking the fluidic channel.

The channel and waveguide are fabricated out of a monolithic fused-silica substrate using a femtosecond laser-writing process combined with chemical etching.

This proof-of-concept device paves the way for more elaborate femtosecond laser-based optofluidic micro-instruments incorporating waveguide networks designed for the real-time field analysis of cells and microorganisms.

3.6. Marking and five dimensional information recordings

The information hunger fuels the race for continuous advances in data storage. Currently, planar technologies are mainly used for this task (magnetic and optical hard disks) with simple multilayering added.

However, increasing storage capacity demands development of new approaches. One of them could be femtosecond laser induced nanogratings, which exhibit anisotropy due to form birefringence. This anisotropy can be characterized by two independent parameters: retardance and slow axis orientation, which can be rewritten with successive pulse sequences. Recently, it was suggested using these parameters to extend optical recording beyond the three dimensions [39]. As a result, femtosecond laser induced self-assembled nanostructures can be employed as a rewritable five-dimensional optical memory.

We explore this technology in depth and demonstrate its actual implementation for multidimensional optical recording and reading.

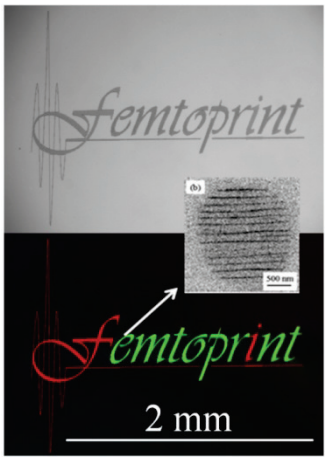

Fig. 15 The Femtoprint project engraved in fused silica. The logo is made using nanogratings arranged spatially so that they introduced a variable retardance that is reflected in the false-image color.

A self-assembled sub-wavelength nanostructure induced in fused silica by femtosecond laser exhibits strong optical anisotropy. This so-called form birefringence can be characterized by retardance and slow axis orientation.

The number of pulses and azimuth of their polarization can independently control these two parameters. The recording of the multiplexed optical memory shown here is performed with a PHAROS mode-locked regeneratively amplified femtosecond laser system (Light Conversion Ltd.) based on a Yb:KGW crystal, operating at $\lambda = 1030$ nm and delivering pulses of 270 fs at a 200 kHz repetition rate. The laser beam is focused with a high-NA lens into the bulk of a fused silica sample mounted on a three-axial motion platform. A successive reading of the recorded information is performed with a quantitative birefringence measurement system (Abrio, Cri Inc.) based on a conventional optical microscope.

As a demonstration of 5D optical writing, we recorded the portraits of two great scientists, Maxwell and Newton, in a piece of silica glass by continuously controlling exposure and polarization during the writing process. The Maxwell portrait was encoded with varying strength of birefringence and Newton's by varying the slow-axis orientation. Later, using the Abrio system, we managed to decouple both images, clearly demonstrating the potential of the proposed information recording technique.

The described memory multiplexing technique by polarization encoding can be successfully applied for high capacity data storage. For instance in the image shown in Fig. 16, we achieved 10 Mb/mm^2 and 1 Gb/mm^3.

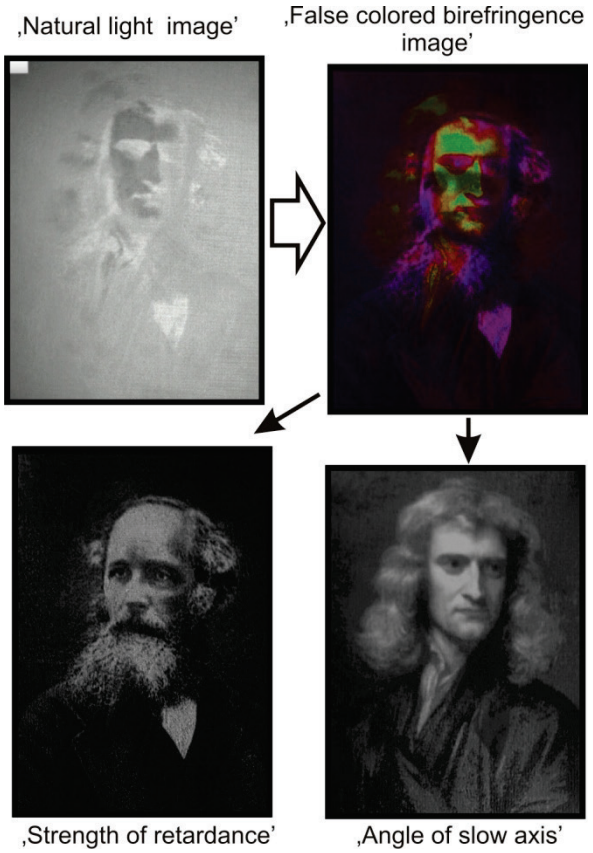

Fig. 16 Example of five dimensional information encoding. The images are 1.5 x 2 mm. The first image (top left) shows the specimen seen under normal lighting conditions. The second image (top right) displays de birefringence information in false colored. The last two images (bottom right, Maxwell and left, Newton) respectively show the decomposed strength of retardance and angle of slow axis information.

3.7. High-speed self-organized bubbles

Depending on the pulse repetition rate, cumulative effects are eventually observed for repetition rates typically above 1 MHz [45],[46].

The formation of organised bubbles trains (nicknamed 'pearl-chains') was reported by R. Graf *et al.* [47] at high-repetition rate, i.e. in the cumulative regime.

We recently demonstrated that such patterns were the outcome of self-organizing patterns emerging from a chaotic behavior [48]. Furthermore, we showed that such patterns can be arranged in 2 or 3 dimensions, forming remarkably cm-long self-organized patterns.

These patterns are obtained by continuously scanning a laser beam across a fused silica specimen in the cumulative regime, rather than using high intensity pulses and high numerical aperture to induce explosions in the material as demonstrated by others.

In the cumulative regime, the formation of bubbles is driven by thermal accumulation effects rather than from micro-explosions as observed with high-focused intensities and high NA [49], [50].

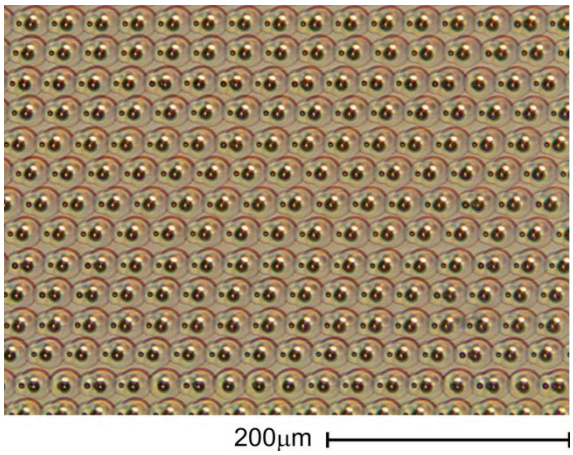

Fig. 17 Two-dimensional grating written in fused silica. Each grating line was written at 30 mm/s. Pulses were fired at 9.4 MHz.

These patterns are obtained at very high scanning rate (>30mm/s) which opens interesting opportunities for mass and high-speed production of self-organized gratings.

4. Outlook

The manufacturing of glass with low-energy femtosecond laser pulses combined with chemical etching defines a flexible manufacturing platform suitable for technologies like optofluidics, optomechanics, marking, and photonics. Through a series of demonstrations, we showed that a laser with small energy requirements (average power of less than a few hundred of milliwatts) can produced complex devices spanning from all-glass actuators and sensors to biochips for algae monitoring and from polarization converters to five dimensional marking. We also demonstrated the use of fused silica substrate as three-dimensional micromolds further expanding the capabilities of this process towards mass-production through polymer replicas.

All these devices and structures can be produced with a table-top production center, nicknamed 'femtoprinter', that costs a fraction of typical investments for micromanufacturing capabilities. We believe that such a system can significantly boost innovation by providing a large pool of users with in-house prototyping and small production capabilities.

Acknowledgments

This project is supported by the European Commission under the 7th Framework Programme under the NMP / Factory of the Future initiative. http://www.femtoprint.eu/

References

[1] T. Kitahara, et al., "Microfactory and microlathe," Int. Workshop on Microfactories, Tsukuba, Japan, pp. 1-8, 7-9 Nov. (1998).

[2] J.-M. Breguet, et al., "Micro/Nanofactory: Concept and state of the art," Conf. on Microrobotics and Microassembly, SPIE vol. 4194, 1-12, 5-6 (2000).

[3] K. M. Davis, K. Miura, N. Sugimoto and K. Hirao, "Writing waveguides in glass with a femtosecond laser," Opt. Lett. 21, 1729-1731 (1996).

[4] A. Marcinkevičius, S. Juodkazis, M. Watanabe, M. Miwa, S. Matsuo, H. Misawa and J. Nishii, "Femtosecond laser-assisted three-dimensional microfabrication in silica," Opt. Lett. **26**, 277-279 (2001).

[5] S. Nolte, M. Will, J. Burghoff, and A. Tuennermann, "Femtosecond waveguide writing: a new avenue to three-dimensional integrated optics," Appl. Phys. A 77, 109-111 (2003).

[6] R. Osellame, N. Chiodo, V. Maselli, A. Yin, M. Zavelani-Rossi, G. Cerullo, P. Laporta, L. Aiello, S. De Nicola, P. Ferraro, A. Finizio, and G. Pierattini, "Optical properties of waveguides written by a 26 MHz stretched cavity Ti:sapphire femtosecond oscillator," Opt. Express **13**, 612-620 (2005).

[7] A. Szameit, D. Blömer, J. Burghoff, T. Schreiber, T. Pertsch, S. Nolte, A. Tünnermann, and F. Lederer, "Discrete Nonlinear Localization in Femtosecond Laser Written Waveguides in Fused Silica," Opt. Express **13**, 10552-10557 (2005).

[8] C. Mauclair, G. Cheng, N. Huot, E. Audouard, A. Rosenfeld, I. V. Hertel, and R. Stoian, "Dynamic ultrafast laser spatial tailoring for parallel micromachining of photonic devices in transparent materials," Opt. Express **17**, 3531-3542 (2009).

[9] L. Canioni, M. Bellec, A. Royon, B. Bousquet, and T. Cardinal, "Three-dimensional optical data storage using third-harmonic generation in silver zinc phosphate glass," Opt. Lett. **33**, 360-362 (2008).

[10] G. Della Valle, S. Taccheo, R. Osellame, A. Festa, G. Cerullo, and P. Laporta, "1.5 μm single longitudinal mode waveguide laser fabricated by femtosecond laser writing," Opt. Express **15**, 3190-3194 (2007).

[11] M. Beresna, M. Gecevicius, P. G. Kazansky, and T. Gertus, "Radially polarized optical vortex converter created by femtosecond laser nanostructuring of glass," Appl. Phys. Lett. 98, 201101–201101 (2011).

[12] D. Psaltis, S.R. Quake, C.H. Yang "Developing optofluidic technology through the fusion of microfluidics and optics," Nature **442,** 381-386 (2006).

[13] Y. Cheng, K. Sugioka, K. Midorikawa, M. Masuda, K. Toyoda, M. Kawachi, and K. Shihoyama, "Three-dimensional micro-optical components embedded in photosensitive glass by a femtosecond laser," Opt. Lett. 28, 1144-1146 (2003).

[14] K. Sugioka, M. Masuda, T. Hongo, Y. Cheng, K. Shihoyama, and K. Midorikawa, "Three-dimensional microfluidic structure embedded in photostructurable glass by femtosecond laser for lab-on-chip applications," Applied Physics A: Materials Science & Processing 79, 815-817 (2004).

[15] Y. Hanada, K. Sugioka, H. Kawano, I. Ishikawa, A. Miyawaki, and K. Midorikawa, "Nano-aquarium for dynamic observation of living cells fabricated by femtosecond laser direct writing of photostructurable glass," Biomedical Microdevices **10**, 403-410 (2008).

[16] Y. Bellouard, A. Said, M. Dugan, and P. Bado, "Fabrication of High-Aspect Ratio, Micro-Fluidic Channels and Tunnels using Femtosecond Laser Pulses and Chemical Etching," Opt. Express **12**, 2120-2129 (2004).

[17] Y. Bellouard, A. Said, M. Dugan, P. Bado, "Monolithic three-dimensional integration of micro-fluidic channels and optical waveguides in fused silica," Materials

Research Society Symposium - Proceedings 782, 63-68 (2003).
[18] A. Schaap, Y. Bellouard, and T. Rohrlack, "Optofluidic lab-on-a-chip for rapid algae population screening," Biomed. Opt. Express 2, 658-664 (2011).
[19] K. Sugioka, Y. Hanada, and K. Midorikawa, "Three-dimensional femtosecond laser micromachining of photosensitive glass for biomicrochips," Laser & Photonics Reviews **4**, 386-400 (2010).
[20] R. Osellame, H. J. W. Hoekstra, G. Cerullo, and M. Pollnau, "Femtosecond laser microstructuring: an enabling tool for optofluidic lab‐on‐chips," Laser & Photonics Reviews **5**, 442-463 (2011).
[21] Y. Bellouard, A. Said, and P. Bado, "Integrating optics and micro-mechanics in a single substrate: a step toward monolithic integration in fused silica," Opt. Express **13**, 6635-6644 (2005).
[22] Y. Bellouard, "On the bending strength of fused silica flexures fabricated by ultrafast lasers," Opt. Mat. Exp., **1** 816-831 (2011).
[23] Y. Bellouard, A. A. Said, M. Dugan, and P. Bado, "Monolithic integration in fused silica: When fluidics, mechanics and optics meet in a single substrate," ISOT - International Symposium on Optomechatronic Technologies (2009), pp. 445-450.
[24] S. Kiyama, S. Matsuo, S. Hashimoto, Y. Morihira, "Examination of Etching Agent and Etching Mechanism on Femotosecond Laser Microfabrication of Channels Inside Vitreous Silica Substrates," The Journal of Physical Chemistry C **113**, 11560-11566 (2009).
[25] C. Hnatovsky, R. S. Taylor, E. Simova, V. R. Bhardwaj, D. M. Rayner, and P. B. Corkum, "Polarization-selective etching in femtosecond laser-assisted microfluidic channel fabrication in fused silica," Opt. Lett. **30**, 1867-1869 (2005).
[26] R. R. Gattass and E. Mazur, "Femtosecond laser micromachining in transparent materials," Nat Photon **2**, 219-225 (2008).
[27] Y. Shimotsuma, P. G. Kazansky, J. Qiu, and K. Hirao, "Self-Organized Nanogratings in Glass Irradiated by Ultrashort Light Pulses," Phys. Rev. Lett. **91**, 247405 (2003).
[28] M. Masuda, K. Sugioka, Y. Cheng, T. Hongo, K. Shihoyama, H. Takai, I. Miyamoto, and K. Midorikawa, "Direct fabrication of freely movable microplate inside photosensitive glass by femtosecond laser for lab-on-chip application," Applied Physics A: Materials Science & Processing **78**, 1029-1032 (2004).
[29] S. Matsuo, S. Kiyama, Y. Shichijo, T. Tomita, S. Hashimoto, Y. Hosokawa, and H. Masuhara, "Laser microfabrication and rotation of ship-in-a-bottle optical rotators," Appl. Phys. Lett. **93**, 051107 (2008).
[30] R. Dorn, S. Quabis, and G. Leuchs, "Sharper focus for a radially polarized light beam," Phys. Rev. Lett. **91**, 233901 (2003).
[31] V. G. Niziev, and A. V. Nesterov, "Influence of beam polarization on laser cutting efficiency," J. Phys. D **32**, 1455-1461 (1999).
[32] F. Xu, R. C. Tyan, P. C. Sun, Y. Fainman, C. C. Cheng, and A. Scherer, "Fabrication, modeling, and characterization of form-birefringent nanostructures," Opt. Lett. **20**, 2457-2459 (1995).
[33] E. Bricchi, B. G. Klappauf, and P. G. Kazansky, "Form birefringence and negative index change created by femtosecond direct writing in transparent materials," Opt. Lett. **29**, 119-121 (2004).
[34] E. Bricchi, J. D. Mills, P. G. Kazansky, B. G. Klappauf, and J. J. Baumberg, "Birefringent Fresnel zone plates in silica fabricated by femtosecond laser machining," Optics letters 27, 2200–2202 (2002).
[35] E. Bricchi, B. G. Klappauf, and P. G. Kazansky, "Form birefringence and negative index change created by femtosecond direct writing in transparent materials," Opt. Lett. 29, 119-121 (2004).
[36] L. Ramirez, M. Heinrich, S. Richter, F. Dreisow, R. Keil, A. V. Korovin, U. Peschel, S. Nolte and A. Tünnermann, 'Tunning the structural properties of femtosecond-laser induced nanogratings', Applied Physics A: Materials Science & Processing **100**, 1-6 (2010).
[37] M. Beresna, and P. G. Kazansky, "Polarization diffraction grating produced by femtosecond laser nanostructuring in glass," Opt. Lett. **35**, 1662-1664 (2010).
[38] Z. Bomzon, V. Kleiner, and E. Hasman, "Formation of radially and azimuthally polarized light using space-variant subwavelength metal stripe gratings," Appl. Phys. Lett. **79**, 1587-1589 (2001).
[39] Y. Shimotsuma, M. Sakakura, P. G. Kazansky, M. Beresna, J. Qiu, K. Miura, and K. Hirao, "Ultrafast Manipulation of Self-Assembled Form Birefringence in Glass, " Adv. Mat. **22** 4039–4043 (2010).
[40] Y. Bellouard, A. Said, M. Dugan, and P. Bado, "Monolithic three-dimensional integration of microfluidic channels and optical waveguides in fused silica," in Materials Research Society Symposium - Proceedings (2003), Vol. 782, pp. 63-68.
[41] A. Schaap, Y. Bellouard, and T. Rohrlack, "Optofluidic lab-on-a-chip for rapid algae population screening," Biomed. Opt. Express **2**, 658-664 (2011).
[42] C. Schaffer, J. García, and E. Mazur, "Bulk heating of transparent materials using a high-repetition-rate femtosecond laser," Appl. Phys., A Mater. Sci. Process. **76**, 351–354 (2003).
[43] S. Rajesh and Y. Bellouard, "Towards fast femtosecond laser micromachining of fused silica: The effect of deposited energy.," Opt. Express **18**, 21490–21497 (2010).
[44] F. Madani-Grasset and Y. Bellouard, "Femtosecond laser micromachining of fused silica molds," Optics Express **18**, 21826–21840 (2010).
[45] C. Schaffer, J. García, and E. Mazur, "Bulk heating of transparent materials using a high-repetition-rate femtosecond laser," Appl. Phys., A Mater. Sci. Process. **76**, 351–354 (2003).
[46] S. Eaton, H. Zhang, P. Herman, F. Yoshino, L. Shah, J. Bovatsek, and A. Arai, "Heat accumulation effects in femtosecond laser-written waveguides with variable repetition rate," Opt. Express **13**, 4708–4716 (2005).
[47] R. Graf, A. Fernandez, M. Dubov, H. J. Brueckner, B. N. Chichkov, and A. Apolonski, "Pearl-chain waveguides written at megahertz repetition rate," Appl. Phys. B **87**, 21-27 (2007).

[48] Y. Bellouard and M.-O. Hongler, "Femtosecond-laser generation of self-organized bubble patterns in fused silica," Opt. Express **19**, 6807-6821 (2011).

[49] E. N. Glezer and E. Mazur, "Ultrafast-laser driven micro-explosions in transparent materials," Appl. Phys. Lett. **71**, 882 (1997).

[50] T. Hashimoto, S. Juodkazis, and H. Misawa, "Void formation in glasses," New Journal of Physics **9**, 253 (2007).

(Received: August 3, 2011, Accepted: December 26, 2011)